



# Parameter value selection strategy for complete coverage path planning based on the Lü system to perform specific types of missions<sup>\*,#</sup>

Caihong LI<sup>†,†1</sup>, Cong LIU<sup>1</sup>, Yong SONG<sup>2</sup>, Zhenying LIANG<sup>1</sup>

<sup>1</sup>School of Computer Science and Technology, Shandong University of Technology, Zibo 255000, China

<sup>2</sup>School of Mechanical, Electrical & Information Engineering, Shandong University (Weihai), Weihai 264209, China

<sup>†</sup>E-mail: lich@sdut.edu.cn

Received May 15, 2022; Revision accepted July 22, 2022; Crosschecked Feb. 9, 2023

**Abstract:** We propose a novel parameter value selection strategy for the Lü system to construct a chaotic robot to accomplish the complete coverage path planning (CCPP) task. The algorithm can meet the requirements of high randomness and coverage rate to perform specific types of missions. First, we roughly determine the value range of the parameter of the Lü system to meet the requirement of being a dissipative system. Second, we calculate the Lyapunov exponents to narrow the value range further. Next, we draw the phase planes of the system to approximately judge the topological distribution characteristics of its trajectories. Furthermore, we calculate the Pearson correlation coefficient of the variable for those good ones to judge its random characteristics. Finally, we construct a chaotic robot using variables with the determined parameter values and simulate and test the coverage rate to study the relationship between the coverage rate and the random characteristics of the variables. The above selection strategy gradually narrows the value range of the system parameter according to the randomness requirement of the coverage trajectory. Using the proposed strategy, proper variables can be chosen with a larger Lyapunov exponent to construct a chaotic robot with a higher coverage rate. Another chaotic system, the Lorenz system, is used to verify the feasibility and effectiveness of the designed strategy. The proposed strategy for enhancing the coverage rate of the mobile robot can improve the efficiency of accomplishing CCPP tasks under specific types of missions.

**Key words:** Chaotic mobile robot; Lü system; Complete coverage path planning (CCPP); Parameter value selection strategy; Lyapunov exponent; Pearson correlation coefficient

<https://doi.org/10.1631/FITEE.2200211>

**CLC number:** TP242.6

## 1 Introduction

The task of complete coverage path planning (CCPP) of a mobile robot is to make the robot cover the whole workplace except obstacles with a low repetition rate or high coverage rate in a given workplace

(Galceran and Carreras, 2013). Currently, this technology has been widely used in commercial robots, such as cleaning (Lakshmanan et al., 2020) and dust removal and mowing (Huang et al., 2021). In addition, there are some robots that perform specific types of missions, such as patrolling (Hoshino and Takahashi, 2019), surveillance (Martins-Filho and Macau, 2007; Curicac and Volosencu, 2014), and demining (Prado and Marques, 2014), which require to not only perform the CCPP task of the whole workplace, but also find intruders and explosives by a random or unpredictable path. The demand for such robots to perform specific types of missions has increased due to the COVID-19 outbreak. This kind of robot, which

<sup>‡</sup> Corresponding author

<sup>\*</sup> Project supported by the National Natural Science Foundation of China (Nos. 61973184 and 61473179) and the Natural Science Foundation of Shandong Province, China (No. ZR2021MF072)

<sup>#</sup> Electronic supplementary materials: The online version of this article (<https://doi.org/10.1631/FITEE.2200211>) contains supplementary materials, which are available to authorized users

ORCID: Caihong LI, <https://orcid.org/0000-0003-0255-9249>

© Zhejiang University Press 2023

can patrol independently, has been introduced in many crowded public places, such as schools, hospitals, stations, sports venues, and customs. People use them for temperature measurement, disinfection, delivery of goods, and guard patrols, which can save manpower and time costs of prevention and control, reduce the possibility of cross infection of epidemic prevention and control staff, and ensure personnel safety effectively.

Mobile robots with chaotic characteristics can meet the need to perform the above specific types of missions. Sekiguchi and Nakamura constructed a chaotic mobile robot using the Arnold system for the first time (Sekiguchi and Nakamura, 1999; Nakamura and Sekiguchi, 2001), where the chaotic characteristics of the system were imparted to the mobile robot to accomplish the CCPP tasks under specific types of missions. The prominent features of chaotic systems are expressed in their topological transitivity and sensitive dependence on the initial conditions, which can meet the requirement of performing the above tasks exactly (Lorenz, 1997; Rajagopal et al., 2020). The characteristic of topological transitivity can ensure that a chaotic robot completely covers the whole patrol area without repetition. The patrol or surveillance robot desires an unpredictable or random trajectory that can be guaranteed by the feature of the sensitive dependence on the initial conditions. Furthermore, a chaotic system is distinct from a random signal. It is unpredictable to the external observer but is also based on determinism, which can be predicted or controlled by the system designer in advance (Li et al., 2019).

The current research idea is to construct a chaotic robot by combining the dynamic system with chaotic characteristics with the kinematic equation of a mobile robot, to generate a complete, random, or unpredictable moving trajectory to meet the requirement of autonomous robots when performing specific types of missions. Many studies have emerged in the past 20 years, among which the work of the Curiac team and Volos team is outstanding. The Curiac team used mainly the chaotic system to monitor specific areas or produce confused positions of obstacles in pursuit missions (Curiac and Volosencu, 2009, 2012, 2014, 2015; Curiac et al., 2018). Curiac and Volosencu (2009) presented a study on the design of two-dimensional

(2D) chaotic trajectories for an intelligent vehicle based on two points of interest that had to be monitored, using a rotation and a scale transformation with the two attractors being placed exactly in the interest positions of the mentioned points. Curiac and Volosencu (2012) used the chaotic Hénon system to produce an unpredictable trajectory to accomplish boundary patrol. The main goal of the bioinspired strategy proposed by Curiac et al. (2018) was to present the varying behavior by changing the reference trajectory suddenly and randomly to perform the overall task of the robot. The above strategy transferred the chaotic characteristics of the 2D Arnold to each reference path segment. The Volos team mainly transformed the chaotic system to a chaotic random bit sequence and sent them to the mobile robot to generate chaotic displacement to accomplish the CCPP task under specific types of missions (Volos et al., 2012a, 2012b, 2012c, 2013; Moysis et al., 2020, 2021; Petavratzis et al., 2020). Volos et al. (2012a, 2012b, 2012c) constructed double-scroll chaotic attractors by a nonlinear circuit to produce the random and chaotic sequences of the mobile robot to accomplish the CCPP task of the entire terrain. Other studies (Volos et al., 2013; Moysis et al., 2020, 2021; Petavratzis et al., 2020) used mainly the logistic map to produce random chaotic bit sequences and convert them to the robot's trajectory to implement a robot's movement in four or eight directions. Fahmy (2012) used a well-known three-dimensional (3D) chaotic system, such as Arnold, Lorenz, and Chua, to construct a chaotic robot combining the chaotic system with the robot kinematic equation. Martins-Filho and Macau (2007) used the Taylor-Chirikov map, also called the standard map, to build a planner of the goal position sequence and impart the chaotic behavior to the mobile robot.

The above research can be roughly divided into two directions. One is to construct a chaotic robot by combining a continuous chaotic system with the dynamic equation of a mobile robot to generate the trajectory performing the CCPP task. The other is to generate a chaotic trajectory by sampling the time series generated by the chaotic equation, which is directly used as the subtarget point during the robot's movement. We have systematically studied the above two strategies regarding how to construct a chaotic

robot and produce the coverage trajectory with a high coverage rate (Li et al., 2015, 2016, 2017, 2018, 2019) based on the chaotic system, such as Logistic, Standard map, Chebychev map, Lorenz, and Arnold. Our research finds that in the latter construction method, it is easy to produce the coverage trajectory with high randomness of a chaotic system. The disadvantage is that the produced trajectory is discrete and likely to change the chaotic performance of the original system. Furthermore, the running environment is fixed in a grid map, and there are only four or eight fixed movements in the map for a robot to choose from. While the first method is the traditional one, which has a complex structure and relatively low randomness, there is no restriction on the running direction of the robot, and it is generated by itself. The produced trajectory is continuous and more in line with the characteristics of a real robot. These two methods are suitable for different applications. Our study is mainly along the first strategy at present.

In addition, most of the current studies use only a set of classical fixed values of the system parameters to construct a chaotic robot. There is also a lack of systematic research on the system parameters and the chaotic and random characteristics of the variables used. Selecting the values of system parameters is a complex problem. The randomness of system variables produced by different values of system parameters is very different; it is also distinct under the same set of values due to sensitivity characteristics. The coverage rates of the trajectory generated by the chaotic robot, which are constructed by different values of parameters and variables, are also different at the same time. Therefore, we study the values of the system parameters and variables for constructing a chaotic robot by a comprehensive selection strategy based on the Lü system. The purpose is to select the optional values of the system parameters and chaotic variables with the best random performance to construct a chaotic robot to produce the trajectory with higher randomness and coverage rate, so that the robot can better accomplish the complete coverage task under specific types of missions. The Lü system comes from the famous Lorenz family, which is similar to the Lorenz system. However, the Lü system has simpler structure with rich dynamic behavior and better chaotic

performance than the Lorenz system (Lü and Chen, 2002).

We analyze the chaotic performance of the Lü system under a set of classical parameters including phase space, phase plane, time series, bifurcation diagram, and Lyapunov exponent. A comprehensive selection strategy is introduced based on the Lü system to gradually determine the optional value range of its parameter. It studies the change in chaotic performance with the parameter varying by analyzing the dissipative system, the Lyapunov exponents, the phase plane, and the Pearson correlation coefficients of the variables. We construct a chaotic robot using chaotic variables and selected values of the system to produce the complete coverage trajectory, and research the influence of the values of the system parameters on the coverage trajectory and the relationship between the sensitive characteristics of the system and the coverage rate of the constructed trajectory. Then we provide the Lorenz system to test and verify the feasibility and effectiveness of the designed comprehensive selection strategy, which is based on the Lü system.

## 2 General analysis of the chaotic performance of the Lü system

The Lü system is a chaotic system proposed by Lü and Chen (2002). Its structure is as follows:

$$\begin{cases} \dot{x} = a(y - x), \\ \dot{y} = cy - xz, \\ \dot{z} = xy - bz, \end{cases} \quad (1)$$

where  $a$ ,  $b$ , and  $c$  are the parameters of the Lü system, and  $x$ ,  $y$ , and  $z$  are the three chaotic variables or system states. Common literature usually takes a set of classical values of system parameters for research, such as  $a=36$ ,  $b=3$ , and  $c=20$  (Mehdi and Kareem, 2017). We analyze the chaotic performance of the Lü system by the phase space, phase plane, time series, and Lyapunov exponent with the values of these parameters and combine qualitative and quantitative methods to analyze the chaotic performance, chaotic degree, and random characteristics of the system.

The 3D phase space is shown in Fig. 1. Fig. S1 (see supplementary materials for Figs. S1–S10) lists three 2D phase planes, and Fig. S2 draws the time series of the three variables, where the initial state  $[x_0, y_0, z_0]=[0, 1, 20]$ , the iteration step  $h=0.01$ , and the number of iterations  $n=10000$ . It can be seen from the phase space and phase planes that the system topologically covers and demonstrates the characteristics of a chaotic attractor. The three variables of the system change with time and show random characteristics (Fig. S2). Fig. S3 shows the part bifurcation diagram (Rabah et al., 2018) regarding the value of parameter  $c$ , where  $c \in [10, 35]$ . It can be seen from the figure that the system changes from period to chaos with varying parameter  $c$ . The above methods qualitatively analyze the chaotic characteristics of the system through graphics.

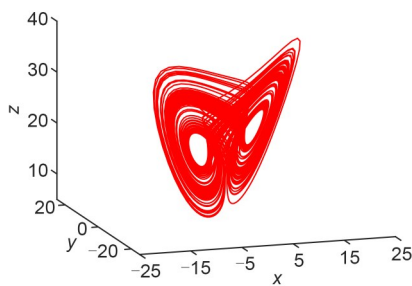


Fig. 1 Phase space (or attractor) of the Lü system

Lyapunov exponent ( $L_E$ ) is one of the most important indices to measure the sensitive dependence on the initial conditions, which is one of the two characteristics of a chaotic system. An  $n$ -dimensional system has  $n$   $L_E$ 's. A system can be concluded to be a chaotic system when the maximum  $L_{E_{\max}}$  is positive (Peitgen et al., 2004).  $L_E$  can be considered the average logarithmic rate of convergence or separation of two adjacent points of two time series  $x_n$  and  $y_n$  separated by an initial distance  $\Delta R_0$ .

$$L_E = \lim_{n \rightarrow \infty} \frac{1}{n} \sum_{i=1}^n \ln \left| \frac{\Delta R_i}{\Delta R_0} \right|, \quad (2)$$

$$\Delta R_0 = \|x_0 - y_0\|_2,$$

where  $i$  is the sequence number of the  $i^{\text{th}}$  value of  $x_n$  and  $y_n$ . When the maximum index  $L_{E_{\max}}$  is positive, the system enters a chaotic state. In general, the greater the value of positive  $L_{E_{\max}}$  is, the larger the

number of positive  $L_E$ 's is, and the better the chaotic performance or randomness of the system is. The three  $L_E$  values of assuming classical system values of the Lü system can be obtained according to the above definition of  $L_E$ :  $L_{E1}=1.898$ ,  $L_{E2}=-0.461$ , and  $L_{E3}=-20.296$ .

Because the maximum exponent  $L_{E1}$  is positive, the Lü equation is concluded to be a chaotic system when assuming the classical values of the parameters  $a=36$ ,  $b=3$ , and  $c=20$ .

### 3 Comprehensive selection strategy for the Lü system

The method of constructing a chaotic robot based on a chaotic system is generally to randomly select a chaotic variable  $x$ ,  $y$ , or  $z$  in the chaotic system, such as the one given by Eq. (1), among a set of fixed classical values. It is the commonly used Lü system. We need to answer the following questions. Does the system have a good chaotic performance under this set of values? Which of the chaotic variables  $x$ ,  $y$ , and  $z$  has the best random characteristics and is more suitable for constructing a chaotic robot? There are many combinations of system parameter values in the optional range. Which combination of them is the best? Which variable is the best in each group? We introduce a comprehensive selection strategy to gradually determine the optional value range of its parameter by analyzing the dissipative system, Lyapunov exponents, phase plane, and Pearson correlation coefficient of the variable based on the extended discussion of the chaotic performance of the Lü system.

#### 3.1 $L_E$ analysis of different parameter values

The values of the two parameters of the Lü system are fixed in the study,  $a=36$ ,  $b=3$ . We discuss the chaotic characteristics, chaotic degree, and variety of  $L_E$  of the system with parameter  $c$  changing to determine its optimal value range, where parameter  $c$  is limited to a positive integer.

##### 3.1.1 Value range of parameter $c$ to ensure a dissipative system

The Lü system belongs to the Lorenz family, and is the first discovered dissipative system that

can show chaotic motion. Its trajectory evolves into an invariant set of attractors over time, thus being a dissipative system. The volume change rate of the phase space is

$$\nabla V = \frac{\partial \dot{x}}{\partial x} + \frac{\partial \dot{y}}{\partial y} + \frac{\partial \dot{z}}{\partial z}. \tag{3}$$

To become a chaotic system,  $\nabla V$  should be smaller than zero. It can be deduced from Eqs. (1) and (3) that

$$\begin{aligned} \nabla V &= \frac{\partial \dot{x}}{\partial x} + \frac{\partial \dot{y}}{\partial y} + \frac{\partial \dot{z}}{\partial z} = -a + c - b \\ &= -36 + c - 3 = -39 + c < 0. \end{aligned}$$

It is deduced that when  $c$  is smaller than 39, the Lü system is a dissipative system and is likely a chaotic attractor. Therefore, the upper limit of parameter  $c$  is roughly determined.

### 3.1.2 $L_E$ research with the Lü system being a dissipative system

We calculate each  $L_E$  of  $c$  when it takes a positive integer less than 39. It is found that when  $c$  assumes a value greater than 35,  $L_E$  cannot be obtained, which indicates that the chaotic characteristics of the system are not significant, so only the values of  $c$  less than or equal to 35 are assumed. When  $c$  is less than 10,  $L_E$  is negative, which does not meet the condition of being a chaotic system. We draw the part  $L_E$  spectrum when  $c \in [10, 35]$ , as shown in Fig. 2.

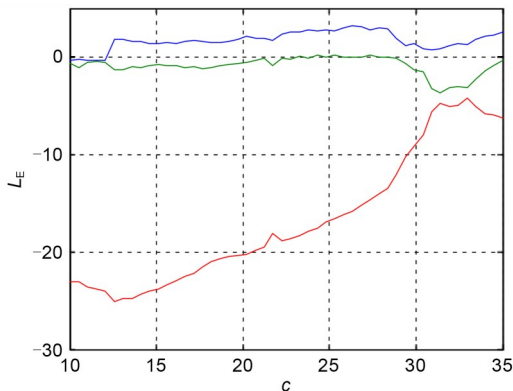


**Fig. 2**  $L_E$  spectrum of the Lü system

The three lines represent the maximum, medium, and minimum indices of  $L_E$  from top to bottom, which are represented by  $L_{E1}$ ,  $L_{E2}$ , and  $L_{E3}$ , respectively

The figure shows that only when parameter  $c$  is greater than 13, is the largest  $L_E$  greater than 0. Then, the value range of parameter  $c$  is further reduced to [14, 35].

### 3.1.3 Analysis of the phase plane

The Lü system remains in a chaotic state as parameter  $c \in [14, 35]$ . When  $c$  takes every integer value, the chaotic characteristics of the system must be different. Some values of the parameter can perform well, while some perform poorly. Which value of system  $c$  has the best chaotic characteristics? Here, we use the phase plane as a tool for qualitative analysis. There are three sets of planes for analysis:  $x-z$ ,  $x-y$ , and  $y-z$ . Because the chaotic properties of the three groups are the same, only one of them is needed.

Fig. S4 illustrates the  $x-z$  phase planes at each integer value of system  $c$ ,  $c \in [14, 35]$ . The topology characteristics of the system are good when  $c \in [20, 28]$ , in which the trajectories are dense and cover the whole workplace. However, others behave worse. Then, the value range of  $c$  is reduced to [20, 28].

### 3.1.4 $L_E$ analysis

Furthermore, we quantitatively analyze the characteristics of each system when  $c \in [20, 28]$ , and calculate each  $L_E$  at every integer value. Table 1 lists all the calculated  $L_E$  values. Table 1 shows that the values of  $L_E$  are different when parameter  $c$  takes different integer values, so the chaotic and random characteristics of the systems are also distinct. In general, the greater the value of positive  $L_E$  and the larger the number of positive exponents, the better the chaotic characteristics of the system. However, when there are two positive  $L_E$ 's in the systems, the chaotic characteristics are affected by both values, so it is difficult to judge which system is better. Table 1 shows that when  $c \in [20, 23]$ , the maximum  $L_E$  of them,  $L_{E1}$ , is not as large as that when  $c \in [24, 28]$ , and each value of the second  $L_E$  of them,  $L_{E2}$ , is negative, so the chaotic performance of the systems when  $c \in [20, 23]$  is not as good as that when  $c \in [24, 28]$ . Therefore, the value range of  $c$  is further reduced to [24, 28].

We can compare the chaotic characteristics when  $c=26$  and 28 according to the two positive  $L_E$ 's in Table 1. The values at  $c=28$  are smaller than their corresponding values at  $c=26$ , indicating that the



chaotic characteristics of the system at  $c=28$  are not as good as those at  $c=26$ . Therefore, the value of  $c=28$  can be removed first, and the range of  $c$  narrows to [24, 27]. For four other values, it is difficult to judge which one has the best performance. Table 1 shows that  $L_{E1}$  varies from small to large, while  $L_{E2}$  changes in the opposite direction, as  $c \in [24, 27]$ . Therefore, it is difficult to judge the random and chaotic results based on the judgment of the two values of  $L_E$ . Furthermore, we combine the Pearson correlation coefficient to judge the random characteristics of the system and variables.

**Table 1**  $L_E$  values when  $c \in [20, 28]$

$c$	$L_{E1}$	$L_{E2}$	$L_{E3}$
20	1.898	-0.461	-20.296
21	2.042	-0.480	-19.465
22	2.185	-0.040	-19.070
23	2.511	-0.016	-18.434
24	2.740	0.207	-17.897
25	2.884	0.170	-17.020
26	3.002	0.132	-16.105
27	3.209	0.002	-15.191
28	2.893	0.054	-13.936

### 3.2 Pearson correlation coefficient

The Pearson correlation coefficient, represented by  $P_{xx'}$ , is a measure of the strength of the linear relationship between two variables  $X$  and  $X'$ , and takes values in the closed interval  $[-1, +1]$ . The smaller the absolute value of  $P_{xx'}$  is, the more irrelevant the two variables  $X$  and  $X'$  are (Profillidis and Botzoris, 2019). Here, we use it to roughly judge the random characteristics of two chaotic variables. Suppose  $X$  is a chaotic variable; then, obtain a variable  $X'$  by increasing a tiny value  $\Delta X$  of  $X$ ,  $X'=X+\Delta X$ .

**Definition 1** If the absolute value of the Pearson correlation coefficient  $|P_{xx'}|$  between chaotic variable  $X$  and its slightly changed variable  $X'$  is very small and tends to zero, the random characteristics of the chaotic variable  $X$  are better.

We design a procedure of calculating the Pearson correlation coefficient of chaotic variables for the Lü system under a set of parameters  $(a, b, c)$ , given an initial value  $(x_0, y_0, z_0)$ , iteration step  $h$ , and number of iterations  $n$ . The length of the obtained time series is  $N=n/h$ . Then, the steps of calculating the Pearson

correlation coefficient of chaotic variable  $X$  are as follows, based on a small change value  $\Delta X$  and variable  $X'$ :

1. Calculate the time series of chaotic variable  $X_i (i=1, 2, \dots, N)$  in Eq. (1) according to a set of given initial values.
2. Calculate the time series of chaotic variable  $X'_i (i=1, 2, \dots, N)$  based on  $X$  and a tiny value  $\Delta X$ .
3. Count the means of the two variables:

$$\begin{cases} \bar{X} = \frac{1}{N} \sum_{i=1}^N X_i, \\ \bar{X}' = \frac{1}{N} \sum_{i=1}^N X'_i. \end{cases} \quad (4)$$

4. Calculate the variances of the two variables:

$$\begin{cases} D(X) = \frac{1}{N} \sum_{i=1}^N (X_i - \bar{X})^2, \\ D(X') = \frac{1}{N} \sum_{i=1}^N (X'_i - \bar{X}')^2. \end{cases} \quad (5)$$

5. Find the covariance of the two variables:

$$\text{Cov}(X, X') = \frac{1}{N} \sum_{i=1}^N (X_i - \bar{X})(X'_i - \bar{X}'). \quad (6)$$

6. Count the Pearson correlation coefficient:

$$P_{xx'} = \frac{\text{Cov}(X, X')}{\sqrt{D(X)D(X')}}. \quad (7)$$

We can calculate the Pearson correlation coefficients of the three chaotic variables  $x, y,$  and  $z$  of Eq. (1) according to the above procedure, where  $\Delta X=0.01$ ,  $a=36$ ,  $b=3$ ,  $c \in [24, 27]$ ,  $h=0.01$ ,  $n=1000$ ,  $N=n/h=100\,000$ ,  $(x_0, y_0, z_0)=(0, 1, 20)$ .

We calculate four sets of absolute values  $P_v$  of the Pearson correlation coefficients of the three chaotic variables  $(x, y, z)$  at each integer value of parameter  $c$  (Table 2), where  $P_{xx'}$ ,  $P_{yy'}$ , and  $P_{zz'}$  are the Pearson correlation coefficients of the three chaotic variables  $x, y,$  and  $z$ , respectively, and  $P_a$  denotes their mean value.

To facilitate comparison, the  $P_v$  values under each group of parameter  $c$  are further given in Fig. 3. It can be seen from Table 2 and Fig. 3 that the  $P_v$  values of the four groups are all small and no more than 0.05,

**Table 2** The absolute values of Pearson correlation coefficients of the variables of the Lü system when  $c \in [24, 27]$

$c$	$P_{xx'}$	$P_{yy'}$	$P_{zz'}$	$P_a$
24	0.0173	0.0171	0.0193	0.0179
25	0.0145	0.0147	0.0198	0.0163
26	0.0375	0.0386	0.0251	0.0337
27	0.0428	0.0406	0.0210	0.0348

which shows that the random performances of the chaotic system are good according to Definition 1. The  $P_v$  values are smaller when  $c$  takes values of 24 and 25, indicating better randomness of chaotic variables. The values at 26 and 27 are larger, and the chaotic performance is relatively poor. The  $P_v$  value is not very accurate, however, because of the sensitive characteristics of chaotic time series. The random performance of variables will not be strictly distinguished when the difference between them is small.

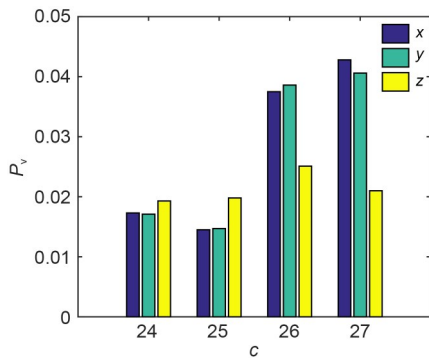


**Fig. 3** Comparison of  $P_v$  of the Lü system

No previous research has pointed out the relationship between the value of the Pearson correlation coefficient  $P_v$  of the chaotic variable and the coverage trajectory generated by the constructed chaotic robot. Of course it is unclear whether the smaller the coefficient is, the better the randomness behaves, and the better the distribution feature of the coverage trajectory is. We use the chaotic robot constructed below to test and verify this relationship.

#### 4 Construction and coverage trajectory analysis of a chaotic robot based on the Lü system

The strategy of constructing the chaotic robot is to select a variable from the three chaotic states in

Eq. (1) and combine it with the robot kinematics equation to transfer the chaotic properties to the robot. The constructed chaotic robot produces a complete coverage trajectory with chaotic properties to accomplish CCPP tasks under specific types of missions. The coverage rate and random performance of its trajectory are evaluated to obtain a better coverage effect.

##### 4.1 Construction of the chaotic robot

A chaotic robot is usually constructed based on the differential structure of a mobile robot. Its kinematic model is

$$\begin{cases} \dot{x}_r = v_r \cos(\theta_r(t)), \\ \dot{y}_r = v_r \sin(\theta_r(t)), \\ \dot{\theta}_r = \omega(t), \end{cases} \quad (8)$$

where  $(x_r, y_r)$  is the position of the robot,  $v_r$  is the velocity of the robot, assumed to be a constant value,  $\theta_r(t)$  is the moving direction of the robot, and  $\omega(t)$  is the angular velocity of the robot.

The chaotic robot can be built in place of  $\theta_r(t)$  in Eq. (8) with a variable chosen from Eq. (1). Suppose that we choose variable  $x$ ; then, the designed chaotic robot is as follows:

$$\begin{cases} \dot{x} = a(y - x), \\ \dot{y} = cy - xz, \\ \dot{z} = xy - bz, \\ \dot{x}_r = v_r \cos x, \\ \dot{y}_r = v_r \sin x. \end{cases} \quad (9)$$

Eq. (9) includes five first-order differential equations embedding the 3D subspace of the Lü system. The chaotic characteristics of the system are imparted to the robot by the chaotic variable  $x$ , which controls its angular velocity. Then, the chaotic coverage trajectory composed of the robot coordinates  $(x_r, y_r)$  is produced step by step, and the CCPP task can be accomplished.

In addition to the five variables in Eq. (9), the Runge–Kutta method is usually used by discretizing the differential equations to find the solution to the robot trajectories. Its common fourth-order model is as follows:

$$\begin{cases} Y_{n+1} = Y_n + \frac{1}{6} (K_1 + 2K_2 + 2K_3 + K_4), \\ K_1 = hf(X_n, Y_n), \\ K_2 = hf(X_n + 0.5h, Y_n + 0.5K_1), \\ K_3 = hf(X_n + 0.5h, Y_n + 0.5K_2), \\ K_4 = hf(X_n + h, Y_n + K_3). \end{cases} \quad (10)$$

Then, four groups of discretization parameters,  $K_1$ ,  $K_2$ ,  $K_3$ , and  $K_4$ , of the differential equations in Eq. (10) are

$$\begin{cases} K_1^x = -ax_n + ay_n, \\ K_1^y = cy_n - x_n z_n, \\ K_1^z = x_n y_n - bz_n, \\ K_2^x = -a\left(x_n + \frac{\Delta t}{2} K_1^x\right) + a\left(y_n + \frac{\Delta t}{2} K_1^y\right), \\ K_2^y = c\left(y_n + \frac{\Delta t}{2} K_1^y\right) - \left(x_n + \frac{\Delta t}{2} K_1^x\right)\left(z_n + \frac{\Delta t}{2} K_1^z\right), \\ K_2^z = \left(x_n + \frac{\Delta t}{2} K_1^x\right)\left(y_n + \frac{\Delta t}{2} K_1^y\right) - b\left(z_n + \frac{\Delta t}{2} K_1^z\right), \\ K_3^x = -a\left(x_n + \frac{\Delta t}{2} K_2^x\right) + a\left(y_n + \frac{\Delta t}{2} K_2^y\right), \\ K_3^y = c\left(y_n + \frac{\Delta t}{2} K_2^y\right) - \left(x_n + \frac{\Delta t}{2} K_2^x\right)\left(z_n + \frac{\Delta t}{2} K_2^z\right), \\ K_3^z = \left(x_n + \frac{\Delta t}{2} K_2^x\right)\left(y_n + \frac{\Delta t}{2} K_2^y\right) - b\left(z_n + \frac{\Delta t}{2} K_2^z\right), \\ K_4^x = -ax_n + ay_n - a\Delta t K_3^x + a\Delta t K_3^y, \\ K_4^y = c\left(y_n + \Delta t K_3^y\right) - \left(x_n + \Delta t K_3^x\right)\left(z_n + \Delta t K_3^z\right), \\ K_4^z = \left(x_n + \Delta t K_3^x\right)\left(y_n + \Delta t K_3^y\right) - b\left(z_n + \Delta t K_3^z\right). \end{cases} \quad (11)$$

Finally, the discrete form of Eq. (9) for the chaotic mobile robot is

$$\begin{cases} x_n = x_{n-1} + \frac{\Delta t}{6} (K_1^x + 2K_2^x + 2K_3^x + K_4^x), \\ y_n = y_{n-1} + \frac{\Delta t}{6} (K_1^y + 2K_2^y + 2K_3^y + K_4^y), \\ z_n = z_{n-1} + \frac{\Delta t}{6} (K_1^z + 2K_2^z + 2K_3^z + K_4^z), \\ x_{r,n} = x_{r,(n-1)} + hv_{r,x} \cos y_n, \\ y_{r,n} = y_{r,(n-1)} + hv_{r,y} \sin y_n, \end{cases} \quad (12)$$

where  $\Delta t$  is the sampling time,  $h$  is the iteration step, and subscript  $n$  indicates the number of iterations. Here,  $\Delta t=1$ ,  $h=0.01$ . Given the initial position  $(x_{r,0}$ ,

$y_{r,0}$ ) of the robot, the initial state  $(x_0, y_0, z_0)$  of the Lü system, and the iteration time  $n_{it}$ , the moving trajectory  $(x_{r,n}, y_{r,n})$  of the robot at any time  $n$  can be obtained. Fig. 4 shows two sets of coverage trajectories produced by the chaotic mobile robot constructed based on Eqs. (11) and (12),  $n_{it}=1000$ . Fig. 4a takes the classical values of system parameters  $a=36$ ,  $b=3$ , and  $c=20$ , while Fig. 4b shows the trajectory when  $c=24$  for comparison. In the figures, curves express the coverage trajectories, and “○” and “◇” show the start point and the end point, respectively. Fig. 4 shows that given an initial state, the chaotic mobile robot can produce a continuous coverage trajectory, and different values of parameter  $c$  of the system can produce completely different coverage trajectories. Similarly, the two other variables  $y$  and  $z$  of the Lü system can be combined with Eq. (8) to construct a chaotic robot. The initial state  $(x_0, y_0, z_0)$  of the Lü system remains unchanged in the following.

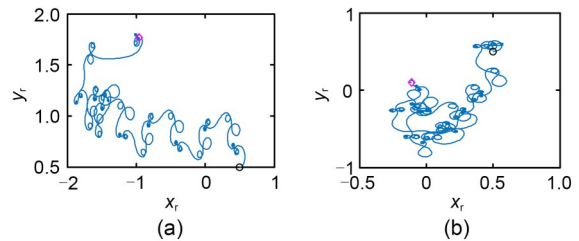
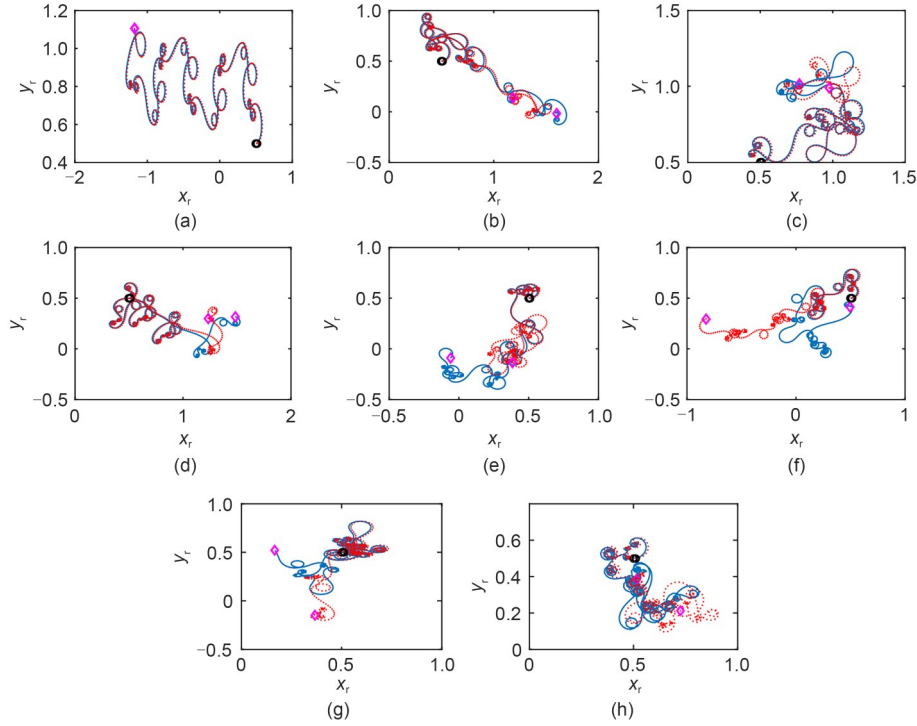


Fig. 4 Coverage trajectories based on the Lü system: (a)  $c=20$ ; (b)  $c=24$

## 4.2 Sensitivity of the chaotic robot to the initial value

We can obtain the coverage trajectories of the constructed chaotic robot according to the different parameters and qualitatively test the sensitivity of the coverage trajectories to the initial values of the robot at specific parameters. Here,  $(x_{r,0}, y_{r,0})=(0.5,0.5)$ . Fig. 5 shows the contrast iteration trajectories by increasing  $x_{r,0}$  with  $\Delta x_{r,0}=0.01$  when  $c \in [20, 27]$ , while the other initial value  $y_{r,0}$  remains unchanged, where the red dotted line is the trajectory after  $x_{r,0}$  changes. The number of iterations  $n_{it}$  takes a smaller value for comparison,  $n_{it}=500$ . Because the start point changes little, the positions of the two start points (marked by ○) basically coincide in the figure. The end points (marked by ◇) of the trajectories basically coincide with the small difference (Fig. 5a) after 500 iterations at  $c=20$ , indicating poor sensitivity. The difference





**Fig. 5** Test of sensitive dependence on the chaotic robot's initial conditions of the coverage trajectory at different values of system  $c$  based on the Lü system: (a)  $c=20$ ; (b)  $c=21$ ; (c)  $c=22$ ; (d)  $c=23$ ; (e)  $c=24$ ; (f)  $c=25$ ; (g)  $c=26$ ; (h)  $c=27$   
References to color refer to the online version of this figure

of the two trajectories becomes increasingly significant after a certain number of iteration steps, showing that the randomness is becoming better from Fig. 5b to Fig. 5e. In Figs. 5e–5h, red dotted lines all change significantly and show that they all have better random characteristics. The above phenomena reflect the changing trend of sensitivity coinciding with the values of  $L_E$  in Table 1. Therefore, we only take the parameters with good sensitivity to construct the chaotic robot, i.e.,  $c \in [24, 27]$ . This is the circumstance caused by chaotic robots constructed by variable  $x$  of the Lü system. The same conclusion can be obtained for the robot constructed with variables  $y$  and  $z$ .

Below we will test whether the chaotic robot system with a high coverage rate can have good randomness.

### 4.3 Coverage performance evaluation of the chaotic robot

Coverage trajectories demonstrate very different performances using different values of the system and state variables produced by the constructed chaotic

robot. Different values of parameters, system start points, and robot start points can produce completely different coverage trajectories under the same system. The evaluation indices of coverage performance include randomness of the coverage trajectory or sensitivity to the initial values, distribution characteristics, and the coverage rate.

#### 4.3.1 Coverage rate

Coverage rate is used to describe the working efficiency of the robot, defined as the ratio of the covered area  $W_c$  to the total workplace  $W_{mn}$ :

$$r_c = \frac{W_c}{W_{mn}}. \quad (13)$$

If a given workspace is quantified as a grid map of equal size,  $r_c$  can be defined as the ratio of the number of grids that have been covered to that of the total ones:

$$r_c = \frac{1}{M} \sum_{i=1}^M G(i), \quad (14)$$

where  $M$  is the total number of grids and  $G(i)$  is the assignment of each grid, having two values:

$$G(i) = \begin{cases} 1, & \text{grid covered,} \\ 0, & \text{grid not covered.} \end{cases} \quad (15)$$

We use the latter method to calculate the coverage rate. Using the state variable with the highest coverage rate to construct a chaotic robot can also produce a trajectory with high performance to improve the working efficiency of the robot.

#### 4.3.2 Static obstacle avoidance

Usually, the robot should work in a fixed workplace, so it is necessary to avoid obstacles along the running boundaries of the robot. At present, the commonly used static obstacle avoidance algorithm for chaotic robots is the mirror mapping algorithm (Nakamura and Sekiguchi, 2001; Fahmy, 2012; Volos et al., 2013; Liu et al., 2017; Li et al., 2019). The working principle is shown in Fig. 6.

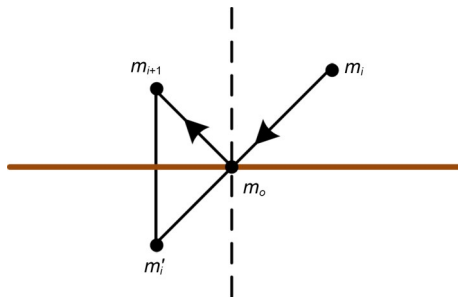


**Fig. 6 Mirror mapping**

The brown bold line is the boundary of the workplace,  $m_i(x_{r,i}, y_{r,i})$  is the current position of the robot,  $m_i'(x_{r,i}, y_{r,i})$  is the next position about to run out of the boundary,  $m_o$  is the collision point between the robot and the boundary, and  $m_{i+1}(x_{r,i+1}, y_{r,i+1})$  is the reflection point of the mirror mapping. References to color refer to the online version of this figure

According to the mirror mapping strategy,  $m_i'$  is reflected back to the workplace, recorded as  $m_{i+1}(x_{r,i+1}, y_{r,i+1})$ , which is the new initial value of the chaotic robot to continue its iteration procedure to accomplish the CCPP task in the given workplace (Li et al., 2019).

We limit the workplace in Fig. 4 to a  $1 \times 1$  size running environment, where the mirror mapping strategy is used for static obstacle avoidance during the robot's

running procedure. Fig. 7 shows the produced trajectories after 5000 iterations at  $c=20$  and 24. The “\*” on the boundaries expresses the mirror reflected points. Calculating them by Eq. (14), the coverage rate of Fig. 7a is 79.5%, while in Fig. 7b it is 91.25%.

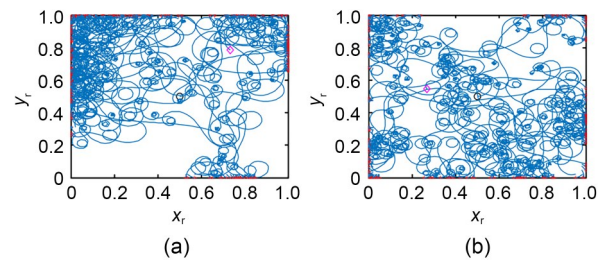


**Fig. 7 Coverage trajectories formed after static obstacle avoidance based on the Lü system: (a)  $c=20$ ; (b)  $c=24$**

#### 4.3.3 Coverage performance evaluation

The initial values of the system remain unchanged. Then, we research the coverage performance of chaotic robots constructed by different values of  $c$  at fixed values of  $a=36$  and  $b=3$ . The trajectory distribution characteristics of most chaotic robots constructed by  $c$  are good when  $c \in [24, 27]$ . When iteration time  $n_{it}=10000$ , most of the coverage rates  $r_c$ 's exceed 90%. Figs. S5–S8 show the coverage trajectories produced by the constructed chaotic robot using three variables  $x$ ,  $y$ , and  $z$ , separately, where the start point of the robot is  $(x_{r,0}, y_{r,0})=(0.5, 0.5)$ . It can be seen that within a certain number of steps, the robot can accomplish the CCPP task.

The coverage rate is also affected by the start point of the robot due to the characteristics of the chaotic system. Different start points lead to different coverage rates, always with great differences. We sample the start point evenly in the workplace within the size of  $1 \times 1$  and take points every 0.01 interval in the horizontal and vertical coordinates to form the size  $99 \times 99$  test points to better compare the performance of the system under each value of  $c$ . Then, we use the three variables under each value of  $c$  to construct the chaotic robot to generate the coverage trajectories at each point, test each coverage rate, and take its mean value for comparison. The test results are shown in Table 3. Fig. 8 lists the values in Table 3 as a histogram.  $c_{xyz}$  is the mean value of the coverage rate of the three variables, and  $f_a$  is the coverage rate of the

trajectory. It can be seen in Table 3 and Fig. 8 that when  $c=24$  and  $25$ , higher coverage rates can be obtained, and the average values exceed 95%. However, when  $c=26$  and  $27$ , the coverage rates are relatively low, below 90%. Comparison of the test results with those in Table 2 and Fig. 3 shows that parameters and variables with better randomness can achieve higher average coverage rates. Therefore, we can select the chaotic parameter variables with good randomness to construct a chaotic robot by analyzing the chaotic and random characteristics of the chaotic system, to increase the coverage rate and the working efficiency of the robot. In total, the value of  $c=24$  or  $25$  is preferred for the Lü system, and it is better to select variable  $x$  or  $y$  of the system to construct a chaotic robot. If the classical value of parameter  $c=20$  is selected to construct a chaotic robot, the randomness of the coverage trajectory is poor, and a high coverage rate cannot be obtained.

**Table 3** The mean coverage rate of the constructed chaotic robot based on the Lü system when  $c \in [24, 27]$

$c$	$x$ (%)	$y$ (%)	$z$ (%)	$c_{xyz}$ (%)
24	97.1	96.5	95.1	96.2
25	97.6	96.6	95.5	96.5
26	88.5	89.1	92.2	89.9
27	83.8	86.9	92.6	87.7

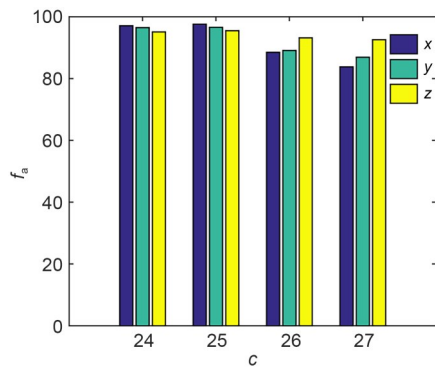


**Fig. 8** Comparison of the mean coverage rate based on the Lü system when  $c \in [24, 27]$

## 5 Test and comparison with the Lorenz system

We test the proposed selection strategy with another chaotic system, the Lorenz system, which was the first chaotic attractor discovered in 1963. It can also be used to construct chaotic robots (Fahmy,

2012; Volos et al., 2012b; Li et al., 2016) to accomplish the CCPP task. The structure of the Lorenz system is as follows:

$$\begin{cases} \dot{x} = a(y - x), \\ \dot{y} = cx - y - xz, \\ \dot{z} = xy - bz, \end{cases} \quad (16)$$

where  $a$ ,  $b$ , and  $c$  are the system parameters that determine the chaotic state and degree of the system. It can be seen from Eq. (16) that the Lorenz system is more complex than the Lü system as given in Eq. (1) as its second differential equation has one more variable.

First, we need to judge how to meet the requirement of being a dissipative system according to the procedure of the designed comprehensive selection strategy. The above conditions can be met as long as parameters  $a$  and  $b$  take positive values, while there is no limit on parameter  $c$ . Suppose that  $a$  and  $b$  take a fixed set of values,  $a=10$ ,  $b=8/3$ . We discuss the chaotic characteristics of the system with change in parameter  $c$  by analyzing the  $L_E$  spectrum of the Lorenz system. It is found that when  $c$  takes an integer greater than 24, there is one and only one  $L_E$  index greater than 0, indicating that the system enters into the chaotic state. By analyzing only the phase planes of the system, such as the Lü system in Fig. S4, the random characteristics with different parameter values of the Lorenz system cannot be distinguished, because their distribution characteristics are similar when  $c$  takes integers greater than 24. Therefore, we only take  $c=25$  and  $28$  for the following research, where  $L_{E1}$ , the largest Lyapunov exponent of  $c=28$ , is greater than that of  $c=25$ , which means that the system of  $c=28$  has better chaotic and random characteristics. Then, a high coverage rate of the trajectory can be obtained by the chaotic robot, constructed by the system of  $c=28$ . Table 4 lists the calculated  $L_E$  when  $c=25$  and  $28$ . The last judgment of the designed strategy is to calculate the Pearson correlation coefficient of the variable under each value of parameter  $c=25$  and  $28$ . Table 5 lists the absolute values of the Pearson correlation coefficients of the Lorenz system variables. We find that variable  $y$  of the Lorenz system has the lowest  $P_v$  value, and  $z$  is the largest. It can be concluded that  $y$  is the most suitable variable for constructing a chaotic robot.

**Table 4**  $L_E$  values of the Lorenz system

$c$	$L_{E1}$	$L_{E2}$	$L_{E3}$
25	0.878	-0.718	-13.741
28	1.138	-0.695	-14.034

**Table 5** The absolute values of the Pearson correlation coefficients of the Lorenz system variables

$c$	$P_{xx'}$	$P_{yy'}$	$P_{zz'}$	$P_a$
25	0.2357	0.2167	0.2478	0.2334
28	0.1916	0.1692	0.2231	0.1946

We discuss the coverage rate constructed by the chaotic Lorenz system when  $c=25$  and  $28$ , in the same simulation environment and test conditions of the Lü system. Figs. S9 and S10 show a set of coverage trajectories, where  $n_{it}=10\,000$  and the start point of the robot is  $(x_{r,0}, y_{r,0})=(0.5, 0.5)$ . Table 6 lists their mean coverage rates.

**Table 6** The mean coverage rate of the constructed chaotic robot based on the Lorenz system

$c$	$x$ (%)	$y$ (%)	$z$ (%)	$c_{xyz}$ (%)
25	67.5	73.9	47.8	63.1
28	75.4	82.9	52.8	70.4

Figs. S9 and S10 and Table 6 show that the chaotic robot constructed by variable  $y$  and  $c=28$  can produce trajectories with a higher coverage rate. These results show that the chaotic variable and system with better random and chaotic characteristics can produce trajectories with a better coverage rate. This is consistent with the conclusion drawn from the Lü system, which shows that the designed selection strategy is feasible and effective. Furthermore, the largest values of  $L_E$  of the Lü system are larger than those of the Lorenz system (as shown in Tables 1 and 4). Therefore, the chaotic and randomness characteristics of the Lorenz system are worse than those of the Lü system, and its coverage rates are also smaller (as shown in Tables 3 and 6 and Figs. S5–S10). This further proves that the parameters and variables with high randomness also have a high coverage rate of the constructed chaotic robot, which can be derived from the designed comprehensive selection strategy.

## 6 Conclusions

We propose a comprehensive selection method for determining the values of parameters and variables of a chaotic system to construct a chaotic robot for the Lü system. It is found that the parameters and variables with high randomness have a high coverage rate of the constructed chaotic robot to perform the CCPP task under specific types of missions. Another chaotic system, the Lorenz system, is used to verify the feasibility and effectiveness of the designed strategy. The proposed algorithm has the following advantages and characteristics:

1. It is easier to generate the coverage trajectory with good randomness and high coverage rate to choose the Lü system as the construction equation of the chaotic robot due to its better chaotic performance and randomness.

2. Combining the deterministic system, phase plane,  $L_E$  index, and Pearson correlation coefficient can gradually reduce the selection range of parameters and finally determine the best values of parameters and variables to construct a chaotic robot with high randomness and coverage rate.

3. The system parameters and variables with a high coverage rate can be chosen by considering only the chaotic characteristics and randomness of the system and variables.

4. This research considers only the selection method of the best values of parameter  $c$ . The selection strategies of two other system parameters  $a$  and  $b$  are basically the same. They can be chosen based on the selected optimal parameter.

5. The system can also obtain better distribution characteristics of individual variables in the positions where the parameter combinations have a lower value of  $L_E$  and the average coverage rate is low. The value of the average coverage rate is basically consistent with that of  $L_E$ .

6. This method is universal. It is applicable not only to Lü and Lorenz systems, but also to Arnold, Rössler, Chua, and other 3D chaotic systems that can be used to construct the chaotic robot to perform the CCPP task.

However, the current research is not perfect. Only when the Pearson correlation coefficient difference is large, can the chaotic time series clearly distinguish

the randomness difference of the system or variable due to the sensitivity of the chaotic system. In addition, when choosing an optimal value of the parameter of a chaotic system, various factors should be comprehensively considered. The chaotic and random characteristics of chaotic time series are affected by the values of the chaotic system parameters, the initial values of the system and robot, etc. Future research should comprehensively consider and study various methods and means to select the appropriate chaotic values of parameters and variables, so that the constructed chaotic robot can better meet the requirements of randomness and distribution characteristics of coverage trajectories to accomplish the CCP task under specific types of missions.

### Contributors

Caihong LI designed the research. Caihong LI and Yong SONG performed the simulations. Caihong LI and Cong LIU implemented the software and drafted the paper. Cong LIU and Zhenying LIANG revised and finalized the paper.

### Compliance with ethics guidelines

Caihong LI, Cong LIU, Yong SONG, and Zhenying LIANG declare that they have no conflict of interest.

### Data availability

Due to the nature of this research, participants of this study did not agree for their data to be shared publicly, so supporting data are not available.

### References

- Curiac DI, Volosencu C, 2009. Developing 2D chaotic trajectories for monitoring an area with two points of interest. Proc 10<sup>th</sup> WSEAS Int Conf on Automation & Information, p.366-369.
- Curiac DI, Volosencu C, 2012. Chaotic trajectory design for monitoring an arbitrary number of specified locations using points of interest. *Math Probl Eng*, 2012:940276. <https://doi.org/10.1155/2012/940276>
- Curiac DI, Volosencu C, 2014. A 2D chaotic path planning for mobile robots accomplishing boundary surveillance missions in adversarial conditions. *Commun Nonl Sci Numer Simul*, 19(10):3617-3627. <https://doi.org/10.1016/j.cnsns.2014.03.020>
- Curiac DI, Volosencu C, 2015. Imparting protean behavior to mobile robots accomplishing patrolling tasks in the presence of adversaries. *Bioinspir Biomim*, 10(5):056017. <https://doi.org/10.1088/1748-3190/10/5/056017>
- Curiac DI, Baniyas O, Volosencu C, et al., 2018. Novel bioinspired approach based on chaotic dynamics for robot patrolling missions with adversaries. *Entropy*, 20(5):378. <https://doi.org/10.3390/e20050378>
- Fahmy AA, 2012. Performance evaluation of chaotic mobile robot controllers. *Int Trans J Eng Manag Appl Sci Technol*, 3(2):145-158.
- Galceran E, Carreras M, 2013. A survey on coverage path planning for robotics. *Robot Auton Syst*, 61(12):1258-1276. <https://doi.org/10.1016/j.robot.2013.09.004>
- Hoshino S, Takahashi K, 2019. Dynamic partitioning strategies for multi-robot patrolling systems. *J Robot Mechatr*, 31(4): 535-545. <https://doi.org/10.20965/jrm.2019.p0535>
- Huang KC, Lian FL, Chen CT, et al., 2021. A novel solution with rapid Voronoi-based coverage path planning in irregular environment for robotic mowing systems. *Int J Intell Robot Appl*, 5(4):558-575. <https://doi.org/10.1007/s41315-021-00199-8>
- Lakshmanan AK, Mohan RE, Ramalingam B, et al., 2020. Complete coverage path planning using reinforcement learning for Tetromino based cleaning and maintenance robot. *Autom Constr*, 112:103078. <https://doi.org/10.1016/j.autcon.2020.103078>
- Li CH, Song Y, Wang FY, et al., 2015. Chaotic path planner of autonomous mobile robots based on the standard map for surveillance missions. *Math Probl Eng*, 2015:263964. <https://doi.org/10.1155/2015/263964>
- Li CH, Song Y, Wang FY, et al., 2016. A bounded strategy of the mobile robot coverage path planning based on Lorenz chaotic system. *Int J Adv Robot Syst*, 13:107. <https://doi.org/10.5772/64115>
- Li CH, Song Y, Wang FY, et al., 2017. A chaotic coverage path planner for the mobile robot based on the Chebyshev map for special missions. *Front Inform Technol Electron Eng*, 18(9):1305-1319. <https://doi.org/10.1631/FITEE.1601253>
- Li CH, Wang ZQ, Fang C, et al., 2018. An integrated algorithm of CCP task for autonomous mobile robot under special missions. *Int J Comput Intell Syst*, 11(1):1357-1368. <https://doi.org/10.2991/ijcis.11.1.100>
- Li CH, Fang C, Wang FY, et al., 2019. Complete coverage path planning for an Arnold system based mobile robot to perform specific types of missions. *Front Inform Technol Electron Eng*, 20(11):1530-1542. <https://doi.org/10.1631/FITEE.1800616>
- Liu P, Sun JJ, Qin HZ, et al., 2017. The area-coverage path planning of a novel memristor-based double-stroll chaotic system for autonomous mobile robots. Chinese Automation Congress, p.6982-6987. <https://doi.org/10.1109/CAC.2017.8244036>
- Lorenz EN, 1997. The Essence of Chaos. Liu SD, translator. China Meteorological Press, Beijing, China, p.186-189 (in Chinese).
- Lü JH, Chen GR, 2002. A new chaotic attractor coined. *Int J Bifurc Chaos*, 12(3):659-661. <https://doi.org/10.1142/S0218127402004620>
- Martins-Filho LS, Macau EEN, 2007. Trajectory planning for surveillance missions of mobile robots. In: Mukhopadhyay SC, Sen Gupta G (Eds.), *Autonomous Robots and Agents. Studies in Computational Intelligence*. Springer, Berlin, Heidelberg, Germany, p.109-117. [https://doi.org/10.1007/978-3-540-73424-6\\_13](https://doi.org/10.1007/978-3-540-73424-6_13)



- Mehdi SA, Kareem RS, 2017. Using fourth-order Runge-Kutta method to solve Lü chaotic system. *Am J Eng Res*, 6(1): 72-77.
- Moysis L, Petavratzis E, Volos C, et al., 2020. A chaotic path planning generator based on logistic map and modulo tactics. *Robot Auton Syst*, 124:103377. <https://doi.org/10.1016/j.robot.2019.103377>
- Moysis L, Rajagopal K, Tutueva AV, et al., 2021. Chaotic path planning for 3D area coverage using a pseudo-random bit generator from a 1D chaotic map. *Mathematics*, 9(15): 1821. <https://doi.org/10.3390/math9151821>
- Nakamura Y, Sekiguchi A, 2001. The chaotic mobile robot. *IEEE Trans Robot Autom*, 17(6):898-904. <https://doi.org/10.1109/70.976022>
- Peitgen HO, Jürgens H, Saupe D, 2004. *Chaos and Fractals: New Frontiers of Science* (2<sup>nd</sup> Ed.). Springer, New York, USA. <https://doi.org/10.1007/b97624>
- Petavratzis E, Moysis L, Volos C, et al., 2020. Chaotic path planning for grid coverage using a modified Logistic-map. *J Autom Mob Robot Intell Syst*, 14(2):3-9. <https://doi.org/10.14313/JAMRIS/2-2020/13>
- Prado J, Marques L, 2014. Energy efficient area coverage for an autonomous demining robot. In: Armada MA, Sanfeliu A, Ferre M (Eds.), *ROBOT2013: First Iberian Robotics Conf: Advances in Intelligent Systems and Computing*. Springer International Publishing, Switzerland, p.459-471. [https://doi.org/10.1007/978-3-319-03653-3\\_34](https://doi.org/10.1007/978-3-319-03653-3_34)
- Profillidis VA, Botzoriz GN, 2019. Statistical methods for transport demand modeling. In: Profillidis VA, Botzoriz GN (Eds.), *Modeling of Transport Demand*. Elsevier, Amsterdam, the Netherlands, p.163-224. <https://doi.org/10.1016/B978-0-12-811513-8.00005-4>
- Rabah K, Ladaci S, Lashab M, 2018. Bifurcation-based fractional-order  $PI^{\alpha}D^{\beta}$  controller design approach for non-linear chaotic systems. *Front Inform Technol Electron Eng*, 19(2):180-191. <https://doi.org/10.1631/FITEE.1601543>
- Rajagopal K, Bayani A, Jafari S, et al., 2020. Chaotic dynamics of a fractional order glucose-insulin regulatory system. *Front Inform Technol Electron Eng*, 21(7):1108-1118. <https://doi.org/10.1631/FITEE.1900104>
- Sekiguchi A, Nakamura Y, 1999. The chaotic mobile robot. *IEEE/RSJ Int Conf on Intelligent Robots and Systems. Human and Environment Friendly Robots with High Intelligence and Emotional Quotients*, p.172-178. <https://doi.org/10.1109/IROS.1999.813000>
- Volos CK, Kyprianidis IM, Stouboulos IN, 2012a. A chaotic path planning generator for autonomous mobile robots. *Robot Auton Syst*, 60(4):651-656. <https://doi.org/10.1016/j.robot.2012.01.001>
- Volos CK, Bardis NG, Kyprianidis IM, et al., 2012b. Implementation of mobile robot by using double-scroll chaotic attractors. *Proc 11<sup>th</sup> Int Conf on Applications of Electrical and Computer Engineering*, p.119-124.
- Volos CK, Kyprianidis IM, Stouboulos IN, 2012c. Motion control of robots using a chaotic truly random bits generator. *J Eng Sci Technol Rev*, 5(2):6-11. <https://doi.org/10.25103/jestr.052.02>
- Volos CK, Kyprianidis IM, Stouboulos IN, 2013. Experimental investigation on coverage performance of a chaotic autonomous mobile robot. *Robot Auton Syst*, 61(12):1314-1322. <https://doi.org/10.1016/j.robot.2013.08.004>

### List of supplementary materials

Fig. S1 Phase planes of the Lü system

Fig. S2 Time series of the Lü system

Fig. S3 Bifurcation diagram regarding the value of parameter  $c$  of the Lü system

Fig. S4 The phase planes of  $x-z$  at each integer value of system  $c$  of the Lü system

Figs. S5–S8 The produced coverage trajectories at  $c=24-27$  based on the Lü system

Figs. S9–S10 The produced coverage trajectories at  $c=25$  and 28 based on the Lorenz system